International Journal of Cardiology xxx (2020) xxx

Contents lists available at ScienceDirect

International Journal of Cardiology

journal homepage: www.elsevier.com/locate/ijcard

Phosphorylated proteome analysis of a novel germline *ABL1* mutation causing an autosomal dominant syndrome with ventricular septal defect

Hidenori Yamamoto [a,1,2], Satoshi Hayano [a,b,1,2], Yusuke Okuno [c,2], Atsuto Onoda [d,e,2], Kohji Kato [f,2], Noriko Nagai [g,2], Yoshie Fukasawa [a,2], Shinji Saitoh [f,2], Yoshiyuki Takahashi [a,2], Taichi Kato [a,*,2]

[a] Department of Pediatrics, Nagoya University Graduate School of Medicine, 65 Tsurumai-cho, Showa-ku, Nagoya, Japan
[b] Department of Pediatrics, Chutoen General Medical Center, 1-1 Shobugaike, Kakegawa, Japan
[c] Center for Advanced Medicine and Clinical Research, Nagoya University Hospital, 65 Tsurumai-cho, Showa-ku, Nagoya, Japan
[d] Division of Neonatology, Center for Maternal-Neonatal Care, Nagoya University Hospital, 65 Tsurumai-cho, Showa-ku, Nagoya, Japan
[e] Faculty of Pharmaceutical Sciences, Sanyo-Onoda City University, 1-1-1 Daigakudori, Sanyo-Onoda, Japan
[f] Department of Pediatrics and Neonatology, Nagoya City University Graduate School of Medical Sciences, 1 Kawasumi, Mizuho-cho, Mizuho-ku, Nagoya, Japan
[g] Department of Pediatrics, Okazaki City Hospital, 3-1 Goshoai, Koryuji-cho, Okazaki, Japan

ARTICLE INFO

Article history:
Received 25 June 2020
Received in revised form 8 October 2020
Accepted 11 October 2020
Available online xxxx

Keywords:
Congenital heart defect
Whole exome sequencing
Phosphorylated proteome analysis
Medical subject headings
Ventricular septal defect

ABSTRACT

Background: A gain-of-function mutation in germline *ABL1* causes a syndrome including congenital heart defects. However, the molecular mechanisms of this syndrome remain unknown. In this study, we found a novel *ABL1* mutation in a Japanese family with ventricular septal defect, finger contracture, skin abnormalities and failure to thrive, and the molecular mechanisms of these phenotypes were investigated.

Methods and results: Whole-exome sequencing on several family members revealed a novel mutation (c.1522A > C, p.I508L) in the tyrosine kinase domain of *ABL1*, and complete co-segregation with clinical presentations was confirmed in all members. Wild-type and mutant *ABL1* were transfected into human embryonic kidney 293 cells for functional analysis. Western blotting confirmed that tyrosine phosphorylation in STAT5, a substrate of ABL1, was enhanced, and the novel mutation was proved to be a gain-of-function mutation. Since this novel mutation in *ABL1* enhances tyrosine kinase activity, phosphorylated proteome analysis was used to elucidate the molecular pathology. The proteome analysis showed that phosphorylation in proteins such as UFD1, AXIN1, ATRX, which may be involved in the phenotypes, was enhanced in the mutant group.

Conclusions: The onset of congenital heart defects associated with this syndrome appears to involve a mechanism caused by UFD1 common to 22q.11.2 deletion syndrome. On the other hand, AXIN1 and ATRX may be important in elucidating the mechanisms of other phenotypes, such as finger contracture and failure to thrive. Verification of these hypotheses would lead to further understanding of the pathophysiology and the development of treatment methods.

1. Introduction

Congenital heart defect (CHD) is one of the major congenital malformations affecting life prognosis, and occurs in about 1 in 100 births [1]. While the prognosis has greatly improved due to recent enhancements in diagnostic and treatment techniques, the underlying etiologies have not been fully elucidated. The cause of most CHD is considered to be multifactorial inheritance because of the interaction of multiple genetic and environmental factors. On the other hand, about 10% of CHD is comprised of single-gene diseases [2]. To date, traditional cloning approaches have identified several disease-causing genes including *NKX2.5*, *GATA4* and *TBX5* [3–5]. Further, in recent years, uncommon genetic mutations responsible for CHD have been identified by whole-exome sequencing (WES). Szot et al. reported a screening approach to detect causative genes using WES in 30 families, including 14 de novo cases, and identified pathogenic variants in 10% (3 families) and additional likely causal variants in 33% (10 families) [6].

ABL1 is a proto-oncogene encoding a tyrosine kinase and is well known to cause chronic myeloid leukemia by forming a fusion gene

Abbreviations: CHD, congenital heart defect; WES, whole-exome sequencing; VSD, ventricular septal defect; HEK, human embryonic kidney; MeSH, Medical subject headings.

* Corresponding author at: Department of Pediatrics, Nagoya University Graduate School of Medicine, 65 Tsurumai-cho, Showa-ku, Nagoya 466-8550, Japan.
E-mail addresses: hy@med.nagoya-u.ac.jp (H. Yamamoto), 3B13624@alumni.tus.ac.jp (A. Onoda), tats1-n@ga2.so-net.ne.jp (N. Nagai), ss11@med.nagoya-cu.ac.jp (S. Saitoh), ytakaha@med.nagoya-u.ac.jp (Y. Takahashi), ktaichi@med.nagoya-u.ac.jp (T. Kato).

[1] These authors contributed equally to this work.
[2] All authors take responsibility for all aspects of the reliability and freedom from bias of the data presented and their discussed interpretation.

https://doi.org/10.1016/j.ijcard.2020.10.032
0167-5273/

with *BCR* in hematopoietic cells, known as the Philadelphia chromosome [7]. The syndrome including CHD caused by germline *ABL1* mutations was identified by using WES in 2017 with two types of missense mutations [8]. The authors reported that the patient with a pathological variant in *ABL1* developed various phenotypes such as skeletal malformations, developmental delay and male genital abnormalities, in addition to CHD. Although it was shown that the variants in *ABL1* cause a gain-of-function in the previous report, the relationship to the phenotypes has not been fully elucidated. In this study, we identified a novel mutation in *ABL1* and investigated the molecular mechanisms using phosphorylated proteome analysis.

2. Material and methods

2.1. Sample collection

This study focused on a Japanese family with autosomal dominant inheritance of ventricular septal defect (VSD), finger contracture, failure to thrive and skin abnormalities, including translucent skin and/or hypopigmentation (Fig. 1). VSD was diagnosed by echocardiography. All living members or their parents provided written informed consent, and their saliva or whole blood was collected. Saliva samples were collected using an Oragene DNA self-collection kit (DNA Genotek, Ottawa, Canada). Genomic DNA was extracted using a QIAamp DNA Blood Mini Kit (Qiagen, Hilden, Germany), according to the manufacturer's instructions. This study was approved by the Ethics Committee of the Nagoya University Graduate School of Medicine (approval number 2015–0032).

2.2. WES analysis

Exome capture was performed on the proband (III:1), his parents (II:2, II:3), and his cousins (III:4, III:5) using SureSelect Human All Exon V5 (Agilent Technologies, Santa Clara, CA), according to the manufacturer's instructions. The generated libraries were sequenced on the HiSeq 2500 platform (Illumina, San Diego, CA). Sequence data were analyzed using an in-house pipeline [9]. Briefly, using the Burrows-Wheeler Aligner [10], the reads were aligned to the UCSC build hg19 reference genome. Picard tools (http://broadinstitute.github.io/picard) were used to remove PCR duplicates. The variants were called using VarScan2, where a variant allele frequency of >0.20 was used as the cutoff value [11]. ANNOVAR was used with in-house scripts to annotate genetic variants [12].

2.3. Mutational analysis

Mutational analysis to define each variant's pathogenicity was essentially based on the latest version of the standards and guidelines for the interpretation of sequence variants issued by the American College of Medical Genetics (ACMG) [13]. Briefly, variants outside of coding regions and variants with >0.1% minor allele frequency in the National Heart, Lung, and Blood Institute ESP (Exome Sequencing Project) 6500 [14], ExAC (Exome Aggregation Consortium) [15], 1000 Genomes Project [16], HGVD (Human Genetic Variation Database) [17], or the in-house database were excluded. Variants that are predicted to cause disorders (e.g., missense variants with reported pathogenicity and nonsense, frameshift insertion/deletion, and splice site variants of genes known to cause disease by inactivation) were verified by Sanger sequencing using PrimeSTAR GXL DNA polymerase (Takara, Shiga, Japan) and a Big Dye Terminator 3.1 Cycle Sequencing Kit (Thermo Fisher Scientific, Waltham, MA) with ABI PRISM 3130xL (Applied Biosystems, Foster City, CA). Primer sequences to verify *ABL1* mutation were as follows: forward primer: 5′- ACCTACTAGAG CGGGACTGG-3′; reverse primer: 5'-CGGAGAAACAGCCCTTAGCA-3′.

2.4. Protein expression

pcDNA3.1^{+}/C-DYK (encoding C-terminal DYK tag), in which wild-type isoform 1b of *ABL1* (NM_007313.2) was cloned, was purchased from GenScript (Piscataway, NJ). Transformation, plasmid purification, and mutagenesis were performed using TOP10 Competent *E. coli* (Thermo Fisher Scientific), QIAprep Spin Miniprep Kit (Qiagen), and KOD-Plus-Mutagenesis Kit (Toyobo, Osaka, Japan), according to the manufacturer's protocol, respectively. The following primers were used for mutagenesis: forward primer: 5′- TTTGCTGAACTCCA CCAAGCCTTTGAAACAATGTT −3′; reverse primer: 5′- GGAGGGCCG GTCAGAGGGATTCCACTGCCA −3′. Sanger sequencing confirmed that the target mutation and no off-target mutations were introduced (Supplementary Fig. 1).

Human embryonic kidney (HEK) 293 cells were cultured in DMEM (Thermo Fisher Scientific) with 10% fetal bovine serum (Thermo Fisher Scientific) at 37 °C under 5% CO_2. Transfection was performed using

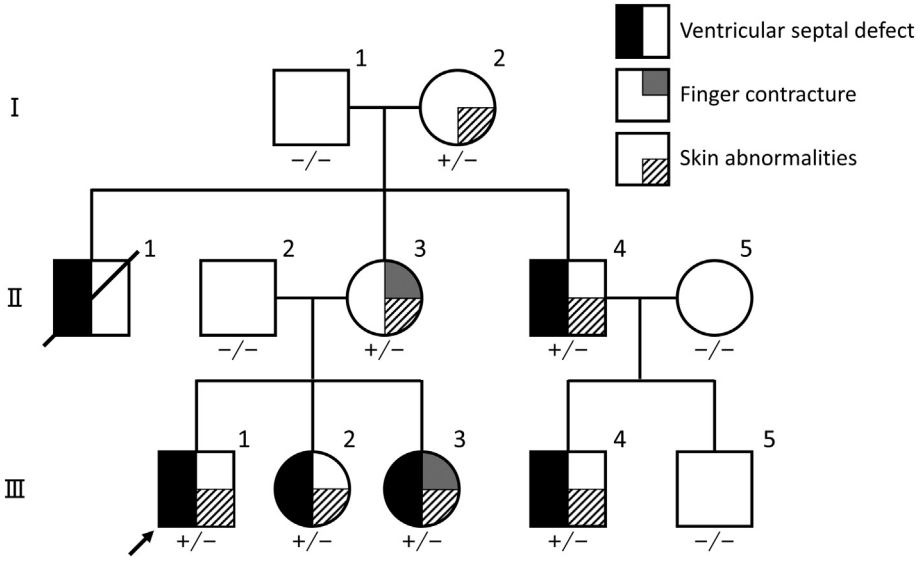

Fig. 1. Pedigree chart of a family with ventricular septal defect, finger contracture, and skin abnormalities, including hypopigmentation and/or translucent skin. Arrow indicates the proband. "+" indicates *ABL1* c.1522A > C mutation positive, and "-" indicates *ABL1* c.1522A > C mutation negative.

Lipofectamine 3000 (Thermo Fisher Scientific) according to the manufacturer's protocol. Total protein was extracted 24 h after transfection using a Detergent-Free Protein Extraction Kit (Invent Biotechnologies, Plymouth, MN) with Phosphatase Inhibitor Cocktail 2 (Sigma-Aldrich, St. Louis, MO) and Complete Protease Inhibitor Cocktail Tablet (Roche, Basel, Switzerland).

2.5. Western blotting

Western blotting was performed in triplicate using JESS technology (Protein Simple, San Jose, CA) with 12–230 kDa Separation Module (Protein Simple), according to the manufacturer's protocol. The primary antibodies were used at the following dilutions: mouse anti-c-Abl (1:50 dilution, Sigma-Aldrich, OP20), rabbit anti-phospho-c-Abl (1:50 dilution, Cell Signaling Technology, Danvers, MA, 2868S), rabbit anti-phospho-STAT5 (1:50 dilution, Cell Signaling Technology, 9359S), mouse anti-phospho-tyrosine (1:1000 dilution, Sigma-Aldrich, 05–321), rabbit anti-actin (1:250 dilution, Sigma-Aldrich, A2066). The dedicated secondary antibodies for anti-mouse and anti-rabbit (Protein Simple) were used without dilution. Digital data was analyzed using Compass software (Protein simple) and normalized by dividing the area value of each protein by the area value of actin. The results were evaluated by a student's *t*-test and were considered statistically significant at $p < 0.05$. The statistical analysis was performed using EZR version 1.37 (Saitama Medical Center, Jichi Medical University, Saitama, Japan), which is a graphic user interface for R (The R Foundation for Statistical Computing, Vienna, Austria) [18].

2.6. Phosphorylated proteome analysis

Phosphorylated proteome analysis was performed using the total HEK 293 protein extracted from 3 samples per group. The proteins were digested by trypsin for 16 h at 37 °C after reduction and alkylation. The phospho-peptides were concentrated using a Titansphere PhosTiO Kit (GL Sciences, Tokyo, Japan) according to the manufacturer's instructions. The phospho-peptides were analyzed by LC-MS using an Orbitrap Fusion mass spectrometer (Thermo Fisher Scientific) coupled to an UltiMate3000 RSLCnano LC system (Dionex Co., Amsterdam, The Netherlands) with a nano HPLC capillary column (150 mm × 75 μm i.d, Nikkyo Technos Co., Tokyo, Japan) via a nanoelectrospray ion source.

Reversed-phase chromatography was performed with a linear gradient (0 min, 5% B; 100 min, 40% B) of solvent A (2% acetonitrile with 0.1% formic acid) and solvent B (95% acetonitrile with 0.1% formic acid) at an estimated flow rate of 300 nL/min. A precursor ion scan was carried out using a 400–1600 mass to charge ratio (*m/z*) prior to MS/MS analysis. Tandem MS was performed by isolation at 0.8 Th with the quadrupole, HCD fragmentation with normalized collision energy of 30%, and rapid scan MS analysis in the ion trap. Only those precursors with charge state 2–6 were sampled for MS2. The dynamic exclusion duration was set to 15 s with 10 ppm tolerance. The instrument was run in top speed mode with 3 s cycles.

2.6.1. Data analysis of phosphorylated proteome analysis

The raw data was processed using either Proteome Discoverer 1.4 (Thermo Fisher Scientific) in conjunction with MASCOT search engine (version 2.6.0, Matrix Science Inc., Boston, MA) for protein identification. Peptides and proteins were identified against the human protein database in UniProt (release 2019_11), with a precursor mass tolerance of 10 ppm, and a fragment ion mass tolerance of 0.8 Da. Fixed modification was set to cysteine carbamidomethylation, and variable modifications were set to methionine oxidation and serine, threonine, tyrosine phosphorylation. Two missed cleavages by trypsin were allowed.

2.6.2. Medical subject headings (MeSH) term analysis

Using the result of proteome analysis, the following method was performed in order to extract the proteins related to the molecular

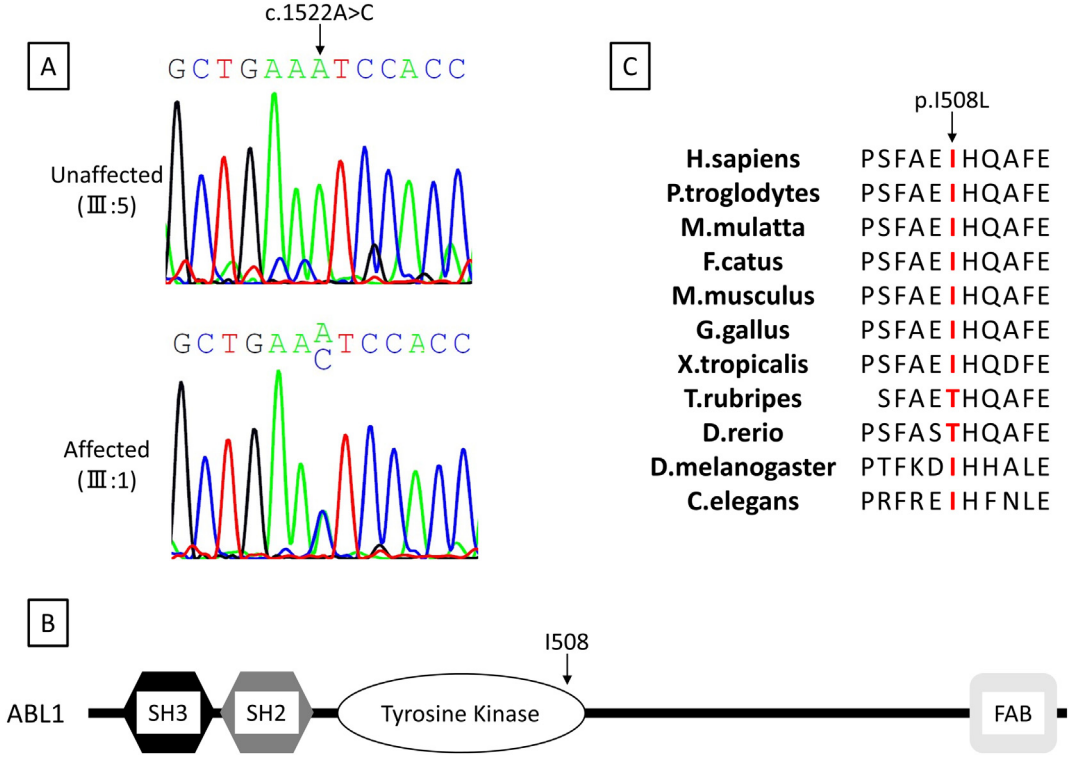

Fig. 2. The novel mutation (c.1522A > C, p.I508L) in *ABL1* (NM_007313.2). A: Sequence chromatograms of unaffected (III:5) and affected (III:1) family members. B: *ABL1* is composed of SH3, SH2, tyrosine kinase and FAB domain, and I508 exists in the tyrosine kinase domain. SH: Src homology domain, FAB: F-actin binding. C: I508 residue is highly conserved among distinct species except for fishes.

mechanisms of phenotype development. At first, among the detected phosphorylated proteins, those with less than the measurement sensitivity in one or more of the six samples were excluded from the viewpoint of reproducibility; whereas, those with less than the sensitivity in only all three samples of one group were judged to be candidate proteins associated with the phenotypes. Subsequently, of the proteins measured in all 6 samples, those with a fold change between the mean of each group >1.5 or < two-thirds were also selected as candidate proteins. From all candidate proteins, those with MeSH terms of $p < 0.05$ in the Gendoo server, which can be openly accessed at http://gendoo.dbcls.jp/, associated with each phenotype were extracted [19]. The following MeSH terms were used for each phenotype: "Heart defects, congenital" for VSD; "limb abnormalities, congenital" and "hand deformities, congenital" for finger contracture; "hypopigmentation" for skin abnormalities; "failure to thrive" for failure to thrive. In order to evaluate the complications frequently reported in the previous study [8], the MeSH terms "intellectual disability" for developmental delay, "urogenital abnormalities" and "hypospadias" for male genital abnormalities were also examined. For the extracted phosphorylated proteins, the *p*-values between the wild-type group and the mutant group were calculated by a student's *t*-test, and the false discovery rates were further calculated using the Benjamini-Hochberg procedure. The false discovery rates were judged to be statistically significant at 0.1 or less.

3. Results

3.1. Clinical features

The proband (III:1) presented with systolic heart murmur and translucent skin. Transthoracic echocardiogram revealed total conus type VSD with enlargement of the left ventricle and atria. Five other family members (II:1, II:4, III:2, III:3, III:4) had also been diagnosed with VSD. VSD of three members (III:2, III:3, III:4) was confirmed to be the subarterial type including total conus defect, and no information was available for the other two members (II:1, II:4). Surgical closure of VSD had been performed for survival on all living members. Finger contracture (Supplementary Fig. 2A), skin abnormalities (Supplementary Fig. 2B), and failure to thrive were diagnosed in two (II:3, III:3), seven (I:2, II:3, II:4, III:1, III:2, III:3, III:4), and five (II:4, III:1, III:2, III:3, III:4) members, respectively. The proband (III:1) also has idiopathic epilepsy without developmental delay. The mother of the proband (II:3) also has Wolff-Parkinson-White syndrome.

3.2. Mutation detection

The number of mutations detected by WES in each sample ranged from 25,155 to 26,105. Five single nucleotide variants and one deletion in a total of five genes that passed the filtering criteria were identified

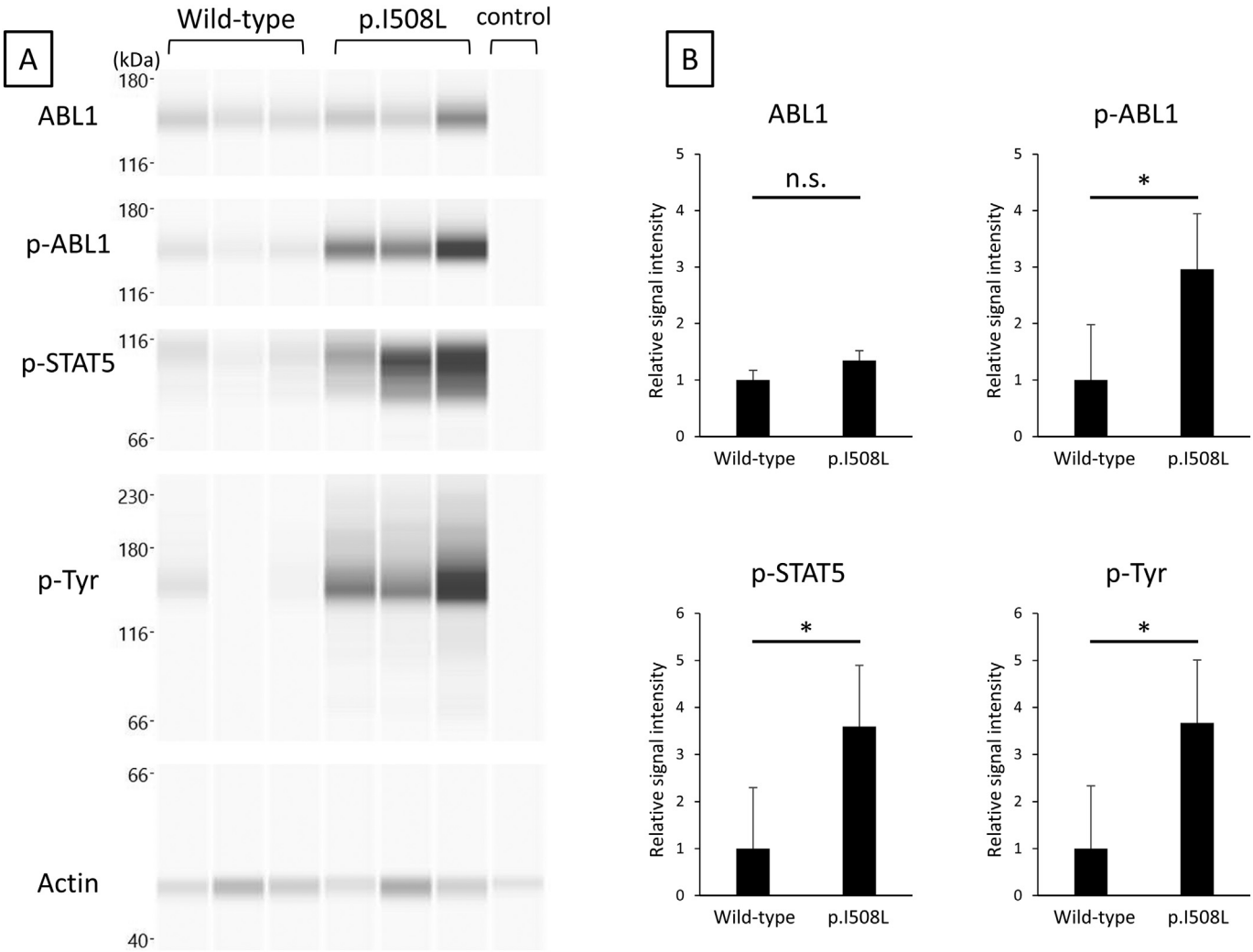

Fig. 3. Functional analysis of the novel variant in *ABL1* by western blotting. A: HEK 293 cells transfected with wild-type and mutant (p.I508L) *ABL1* in three samples per group were used. HEK 293 cells not transfected with any vector were used as the negative control. B: The values corrected by actin were compared. Phospho-ABL1, phospho-STAT5, and the overall expression of phospho-tyrosine were significantly increased in the mutant group. HEK: human embryonic kidney. *: $p < 0.05$, n.s.: $p > 0.05$.

(Supplementary Table 1). A novel nonsynonymous variant c.1522A > C (p.I508L) in *ABL1* segregated with complete penetrance in all family members, which was confirmed by Sanger sequencing (Fig. 2A). The amino acid change was predicted to be tolerated with a score of 0.12, possibly damaging with a score of 0.469, deleterious with a score of zero, and disease causing by SIFT, Polyphen2, LRT, and MutationTaster, respectively. In addition, the I508 residue in *ABL1* is located in the tyrosine kinase domain and is relatively highly conserved among distinct species except for fishes (Fig. 2B, C). The other four genes containing passed mutations were investigated against the published literature and no phenotype-associated reports were found.

3.3. Western blotting

Results of the protein expression analysis of wild-type and mutant (p.I508L) *ABL1* using HEK 293 cells revealed that phospho-ABL1, phospho-STAT5, and the overall expression of phospho-tyrosine were significantly increased in the mutant group compared to the wild-type group (Fig. 3). This proved that p.I508L in *ABL1* caused a gain-of-function mutation.

3.4. Phosphorylated proteome analysis

Extraction of the phosphorylated proteins possibly related to the molecular mechanisms of the phenotypes is shown in Fig. 4. Among 2403 measured phosphorylated proteins, 1146 were measured in all 6 samples, and 894 (78%) of them tended to show enhanced phosphorylation in the mutant group, as shown by the volcano plot in Supplementary Fig. 3. The fold changes between the wild-type and mutant groups were > 1.5 or < two-thirds in 242 proteins, and 232 (92%) of them tended to show enhanced phosphorylation in the mutant group. Proteins that could be measured in only three samples of the wild-type group or mutant group were 2 and 37, respectively. Among the total 281 candidate proteins possibly associated with the phenotypes, the number of proteins with the MeSH terms for VSD, finger contracture, skin abnormalities, failure to thrive, developmental delay and male genital abnormalities were 6, 13, 1, 2, 11 and 4, respectively. Among them, the proteins showing significant changes for each phenotype were as follows: HSPA1A, MED1 and UFD1 for VSD; TRIP6, EWSR1 and AXIN1 for finger contracture; ZMYM3 for skin abnormalities; ATRX for failure to thrive; HINT1 and ATRX for developmental delay; ATRX, FKBP4, DBNL and AXIN1 for male genital abnormalities (Supplementary Table 2).

4. Discussion

In this study, we identified a novel gain-of-function mutation (p.I508L) in *ABL1* in a family with an autosomal dominant inherited syndrome including VSD. Using phosphorylated proteome analysis, we also showed that this novel mutation enhances phosphorylation of phenotype-related proteins.

Although this syndrome has been reported in three papers in the past [8,20,21], the present study has two novelties. First, the present reported family is the largest one with confirmed genetic mutations in seven members, which may suggest that the phenotype and its severity differ due to the variant. Previous reports have confirmed *ABL1* mutation in 13 patients, including 2 familial cases, but most cases are de novo cases. One of the reasons why this family could become a large pedigree may be that their phenotypes were milder than previously reported patients. Previously reported patients frequently developed

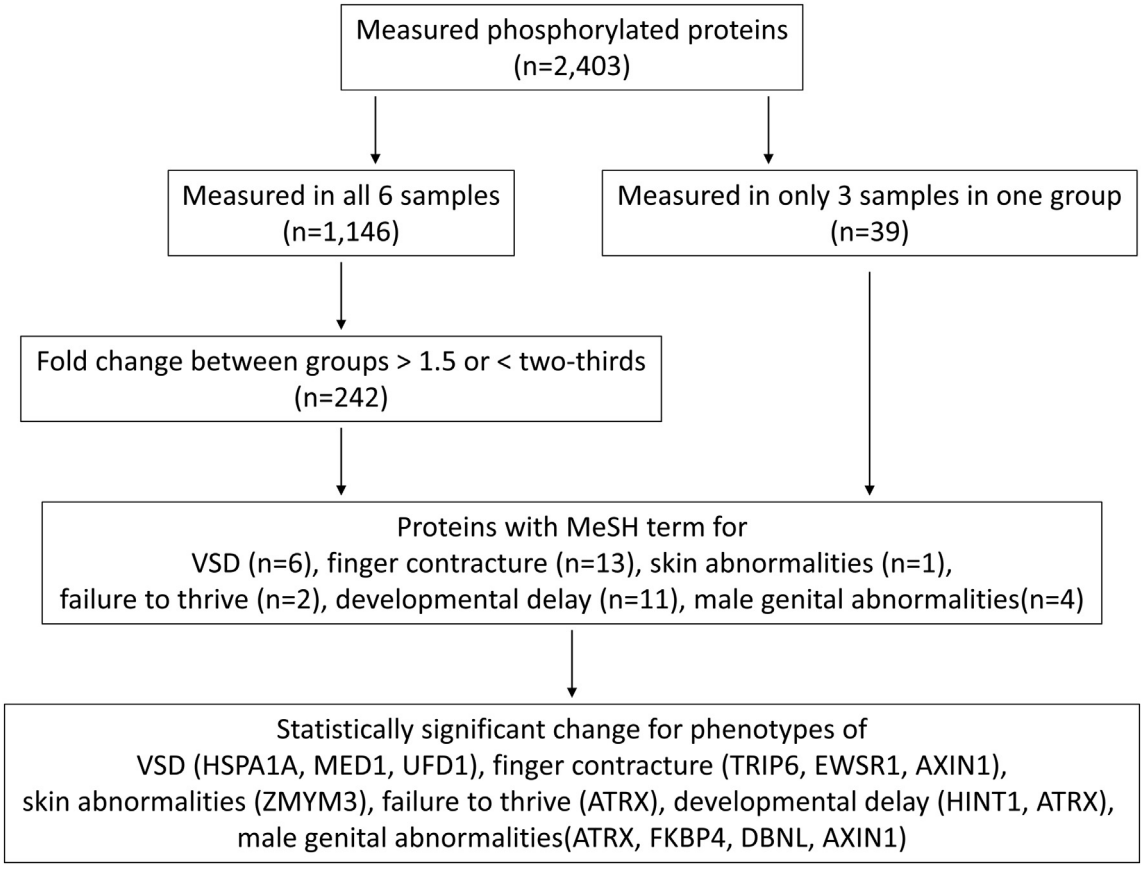

Fig. 4. Method used to extract phosphorylated proteins related to the molecular mechanisms of the phenotypes. Among the proteins measured by phosphorylated proteome analysis, those potentially related to the molecular mechanism for each phenotype were extracted. MeSH: medical subject headings, VSD: ventricular septal defect.

phenotypes that can affect social adaptation and reproduction, such as developmental delay and male genital abnormalities, respectively. On the other hand, the present reported family members with the variant in *ABL1* required no intervention other than for CHD, and all were able to adapt to society normally. Regarding CHD, there were some moderately complex types such as tetralogy of Fallot in the previous reports, but in the present patients, only the simple type, that is, VSD, was present. These facts may suggest that the phenotypes and the severity of this syndrome differ depending on the site of the variant.

As a second novelty, the molecular mechanism of this syndrome was investigated using phosphorylated proteome analysis, and proteins that may be phenotypically relevant were present. Although it has been proven that each germline *ABL1* variant in the previous reports was a gain-of-function mutation, as described above, the causal relationship between the mutation and phenotypes has not been proven. Our study is the first report to analyze the molecular mechanisms between the mutation and phenotypes. Of the three proteins with the MeSH term "heart defects, congenital", UFD1 is known as one of the candidate genes for 22q.11.2 deletion syndrome, and it has been reported in an animal experiment that a loss-of-function of the gene causes congenital heart defects [22]. Most of the CHD in 22q.11.2 deletion syndrome is accompanied by outflow tract abnormalities such as tetralogy of Fallot and aortic arch anomalies [23]. Cardiovascular abnormalities, including dilation of the sinus of Valsalva, were found in 11 patients with *ABL1* variant in previous reports, eight of which were associated with some outflow tract abnormalities. In addition, the CHD in the present reported members was VSD in all cases, but it is very characteristic that all were the subarterial type including a total conus defect. These findings may support the existence of a mechanism of developing CHD common to this syndrome and to 22q.11.2 deletion syndrome.

Next, let us consider proteins with the MeSH terms other than "heart defects, congenital". *ATRX* is located on the long arm of the X chromosome, and abnormalities of this gene have been suggested to be involved in male genital abnormalities and growth and developmental delay. Furthermore, it has been reported that abnormalities of this gene were also involved in skeletal abnormalities in the face or trunk [24]. On the other hand, AXIN1 is known to inhibit cartilage formation via inhibition of Wnt/beta-catenin signaling [25]. These proteins may be involved in the development of each phenotype of this syndrome, and regulation of these proteins in patients may be therapeutic targets. As an issue for future investigation, in vivo studies using knock-in mice are needed to verify this hypothesis. On the other hand, our study was not able to show a relationship with skin abnormalities. It is possible that one of the reasons may be the use of HEK 293 cells which are derived from the fetal kidney. In this respect as well, re-examination is desired in studies using knock-in mice.

5. Conclusion

It was suggested that a gain-of-function mutation of *ABL1* in germline cells exhibits several phenotypes including CHD through phosphorylation of various proteins, such as UFD1, AXIN1, and ATRX.

Supplementary data to this article can be found online at https://doi.org/10.1016/j.ijcard.2020.10.032.

Authors' contributions

H.Y., S·H, and T.K. contributed to the conception and design of this study; S.H. and N.N. analyzed the clinical data; H.Y., S.H., Y.O., A.O., and K.K. performed the experiments and analyzed the data; Y.F., S.S., Y.T., and T.K. critically reviewed the manuscript. All authors approved the final version of the manuscript.

Sources of funding

This work was supported by the Japan Society for the Promotion of Science KAKENHI Grant No. 19 K17357 and 19 K08319.

Declaration of Competing Interests

The authors have no conflict of interest to declare.

Acknowledgements

The authors wish to acknowledge the Division for Medical Research Engineering, Nagoya University Graduate School of Medicine for technical support in next-generation sequencing and proteome analysis. The authors also acknowledge the assistance of the Human Genome Center, Institute of Medical Science, University of Tokyo (http://sc.hgc.jp/shirokane.html) for providing supercomputing resources.

References

[1] L.D. Botto, Epidemiology and prevention of congenital heart defects, in: H.D. Allen (Ed.), Moss and Adams' Heart Disease in Infants, Children, and Adolescents Including the Fetus and Young Adult, 9th ednWolters Kluwer, Philadelphia, PA 2016, pp. 55–86.
[2] E. Goldmuntz, M.L. Crenshaw, Genetic aspects of congenital heart defects, in: H.D. Allen (Ed.), Moss and Adams' Heart Disease in Infants, Children, and Adolescents Including the Fetus and Young Adult, 9th ednWolters Kluwer, Philadelphia, PA 2016, pp. 87–116.
[3] J.J. Schott, D.W. Benson, C.T. Basson, et al., Congenital heart disease caused by mutations in the transcription factor NKX2-5, Science. 281 (1998) 108–111, https://doi.org/10.1126/science.281.5373.108.
[4] V. Garg, I.S. Kathiriya, R. Barnes, et al., GATA4 mutations cause human congenital heart defects and reveal an interaction with TBX5, Nature. 424 (2003) 443–447, https://doi.org/10.1038/nature01827.
[5] C.T. Basson, D.R. Bachinsky, R.C. Lin, et al., Mutations in human TBX5 [corrected] cause limb and cardiac malformation in Holt-Oram syndrome, Nat. Genet. 15 (1997) 30–35, https://doi.org/10.1038/ng0197-30.
[6] J.O. Szot, H. Cuny, G.M. Blue, et al., A screening approach to identify clinically actionable variants causing congenital heart disease in exome data, Circ Genom Precis Med. 11 (2018), e001978, https://doi.org/10.1161/CIRCGEN.117.001978.
[7] R. Rau, M.L. Loh, Myeloproliferative neoplasms of childhood, in: P.A. Pizzo, D.G. Poplack (Eds.), Principles and Practice of Pediatric Oncology, 7th ednWolters Kluwer, Philadelphia 2016, pp. 545–567.
[8] X. Wang, W.L. Charng, C.A. Chen, et al., Germline mutations in ABL1 cause an autosomal dominant syndrome characterized by congenital heart defects and skeletal malformations, Nat. Genet. 49 (2017) 613–617, https://doi.org/10.1038/ng.3815.
[9] H. Muramatsu, Y. Okuno, K. Yoshida, et al., Clinical utility of next-generation sequencing for inherited bone marrow failure syndromes, Genet Med. 19 (2017) 796–802, https://doi.org/10.1038/gim.2016.197.
[10] H. Li, R. Durbin, Fast and accurate short read alignment with Burrows-Wheeler transform, Bioinformatics. 25 (2009) 1754–1760, https://doi.org/10.1093/bioinformatics/btp324.
[11] D.C. Koboldt, Q. Zhang, D.E. Larson, et al., VarScan 2: somatic mutation and copy number alteration discovery in cancer by exome sequencing, Genome Res. 22 (2012) 568–576, https://doi.org/10.1101/gr.129684.111.
[12] K. Wang, M. Li, H. Hakonarson, ANNOVAR: functional annotation of genetic variants from high-throughput sequencing data, Nucleic Acids Res. 38 (2010), e164, https://doi.org/10.1093/nar/gkq603.
[13] S. Richards, N. Aziz, S. Bale, et al., Standards and guidelines for the interpretation of sequence variants: a joint consensus recommendation of the American College of Medical Genetics and Genomics and the Association for Molecular Pathology, Genet Med. 17 (2015) 405–424, https://doi.org/10.1038/gim.2015.30.
[14] Exome Variant Server, NHLBI GO Exome Sequencing Project (ESP), Seattle, WA http://evs.gs.washington.edu/EVS/ Accessed date: 1 June 2020.
[15] M. Lek, K.J. Karczewski, E.V. Minikel, et al., Analysis of protein-coding genetic variation in 60,706 humans, Nature. 536 (2016) 285–291, https://doi.org/10.1038/nature19057.
[16] 1000 Genomes Project Consortium, Auton A, Brooks LD, et al, A global reference for human genetic variation, Nature 526 (2015) 68–74, https://doi.org/10.1038/nature15393.
[17] K. Higasa, N. Miyake, J. Yoshimura, et al., Human genetic variation database, a reference database of genetic variations in the Japanese population, J. Hum. Genet. 61 (2016) 547–553, https://doi.org/10.1038/jhg.2016.12.
[18] Y. Kanda, Investigation of the freely available easy-to-use software 'EZR' for medical statistics, Bone Marrow Transplant. 48 (2013) 452–458, https://doi.org/10.1038/bmt.2012.244.
[19] T. Nakazato, H. Bono, H. Matsuda, T. Takagi, Gendoo: functional profiling of gene and disease features using MeSH vocabulary, Nucleic Acids Res. 37 (2009) W166–W169, https://doi.org/10.1093/nar/gkp483 Web Server issue.

[20] N. Bravo-Gil, I. Marcos, A. González-Meneses, G. Antiñolo, S. Borrego, Expanding the clinical and mutational spectrum of germline ABL1 mutations-associated syndrome: A case report, Medicine (Baltimore) 98 (2019) e14782, https://doi.org/10.1097/MD.0000000000014782.

[21] C.A. Chen, E. Crutcher, H. Gill, et al., The expanding clinical phenotype of germline ABL1-associated congenital heart defects and skeletal malformations syndrome, Hum Mutat (2020)https://doi.org/10.1002/humu.24075.

[22] C. Yamagishi, B.P. Hierck, A.C. Gittenberger-De Groot, H. Yamagishi, D. Srivastava, Functional attenuation of UFD1l, a 22q11.2 deletion syndrome candidate gene, leads to cardiac outflow septation defects in chicken embryos, Pediatr. Res. 53 (2003) 546–553, https://doi.org/10.1203/01.PDR.0000055765.11310.E3.

[23] E. Goldmuntz, M.L. Crenshaw, Genetic aspects of congenital heart defects, in: H.D. Allen (Ed.), Moss and Adams' Heart Disease in Infants, Children, and Adolescents Including the Fetus and Young Adult, 9th ednWolters Kluwer, Philadelphia, PA 2016, pp. 87–116.

[24] D. Lugtenberg, A.P. de Brouwer, A.R. Oudakker, et al., Xq13.2q21.1 duplication encompassing the ATRX gene in a man with mental retardation, minor facial and genital anomalies, short stature and broad thorax, Am. J. Med. Genet. A 149A (2009) 760–766, https://doi.org/10.1002/ajmg.a.32742.

[25] D.Y. Dao, X. Yang, D. Chen, M. Zuscik, R.J. O'Keefe, Axin1 and Axin2 are regulated by TGF- and mediate cross-talk between TGF- and Wnt signaling pathways, Ann. N. Y. Acad. Sci. 1116 (2007) 82–99, https://doi.org/10.1196/annals.1402.082.